OPENQUATERNARY

Ermertz, AM, et al. 2019. Geoarchaeological Evidence for the Decline of the Medieval City of Qalhat, Oman. *Open Quaternary*, 5: 8, pp. 1–14. DOI: https://doi.org/10.5334/oq.56

RESEARCH PAPER

Geoarchaeological Evidence for the Decline of the Medieval City of Qalhat, Oman

Alina Marie Ermertz[*,†], Miklos Kázmér[‡,§], Silja Kerstin Adolphs[*], Michaela Falkenroth[*] and Gösta Hoffmann[*,‖]

The medieval city of Qalhat was an important trade town along the sea routes in the Indian Ocean. The reasons for the decline of the city are unclear, as the archaeological evidence is inconclusive. Geological field work was conducted and a digital elevation model analysed to test the hypothesis that the city was destroyed by an earthquake. The study area is located along the passive continental margin of the Arabian Plate. The coast shows a set of Pleistocene marine terraces. These landforms are in indication of lithosphere uplift. Faulted terrace fill deposits and deviating fluvial streams indicate rather recent lithosphere deformation. Processes responsible for the deformation are seen as subduction related forebulge uplift, serpentinite diapirism as well as isostatic response to karstification of limestone. We conclude that earthquake activity along the most prominent structural element, the Qalhat Fault, is a plausible reason for the decline of the medieval city.

Keywords: neo-tectonics; earthquake; Qalhat; marine terraces; crustal deformation; serpentinite

Introduction and Aims

The city of Qalhat is located on the coastline of Oman. The coastal geomorphology of the shorelines of the northern Indian Ocean in Oman is divers: large beaches characterise the distal parts of alluvial fans in the north of the country, whereas rocky coastlines dominate along the eastern coast where the mountains are close to the sea. The coastal zone of Oman is an area of preferred settlement mainly for climatic and economic reasons. In contrast to the interior of the country where arable land is scarce, agriculture is possible within the coastal zone due to exploitation of a shallow aquifer. A further benefit is the access to food resources including sea food. There is evidence that human occupation along the coastline under study goes back to the Early Bronze Age (Giraud 2009). Geological and archaeological research projects currently concentrate on the quantification of coastal dynamics including short term sea level changes in form of tsunami (e.g. Hoffmann et al. 2013) and storm surges (e.g. Fritz et al. 2010), tectonically induced long term vertical crustal uplift (e.g. Moraetis et al. 2018, Falkenroth, Schneider & Hoffmann 2019) as well as the settlement history (e.g. Rose et al. 2019).

Globally, the access to trade routes is another reason for the socio-economic importance of the coast. As a consequence, important cities developed in various places along the world's shorelines, especially along major maritime trading routes. This holds true for the Indian Ocean as well (Hourani & Carswell 1995). Trade routes connecting Africa, India and Arabia are of historical importance along the coastline of Oman (Boivin & Fuller 2009). One of the cities that gained importance in the Indian Ocean trade is Qalhat, located near the city of Sur along the coastline of Oman on the shores of the Indian Ocean. The history of Qalhat is very poorly documented (Bhacker & Bhacker 2004) and its rise and fall has often been perceived as a mystery. Apparently, it emerged as a prosperous seaport in the 12th century AD as part of the Hormuz dynasty. The 13th and 14th century AD are known as the golden era (Ibrahim & El Mahi 2000) when the city was an important administrative and political hub (Agius 1999). This medieval seaport was the chief port of trade along the Omani seaboard, and was the most important port-of-call situated on the main sea route from India to Persia and the Gulf (Bhacker & Bhacker 2004). Foreign control came with the Portuguese who arrived in 1507 AD. At that time the city was already in decline. The reasons are unknown; however, speculations include natural reasons such as an earthquake or a tropical cyclone in the last quarter of the 15th century AD (Bhacker & Bhacker 2004). The city was finally pillaged and looted by Portuguese troops in AD 1508. It soon lost its importance and Muscat became the most important port.

* Institute of Geosciences, Bonn University, Nussallee 8, Bonn, DE

† Federal Institute for Geosciences and Natural Resources (BGR), Stilleweg 2, Hannover, DE

‡ Department of Paleontology, Eötvös University, Pázmány Péter sétány 1/c, Budapest, HU

§ MTA-ELTE Geological, Geophysical and Space Science Research Group, Budapest, HU

‖ Institute of Neotectonics and Natural Hazards, RWTH Aachen University, Aachen, DE

Corresponding author: Alina Marie Ermertz (alina.ermertz@bgr.de)

The old city of Qalhat is a protected archaeological site that was recently registered in the world heritage list by the UNESCO. The city covers an area of approximately 35 ha. Already surficial pottery testifies that the city was an important trade town. Abundant shards document trade connections to Asia and Africa. Excavations are ongoing since 2003. Rubble of ruined buildings and lanes are located on a coastal headland situated at a wadi mouth at the foot of a mountain at elevations of 0 to 30 m above mean sea level. The site represents a walled medieval settlement, triangular in shape, confined and protected by natural features such as a wadi, the sea and a steep mountain front. Archaeological remains clearly identify the town as of significance and wealth, a fact which is further stressed by the heavily fortified character of the settlement. The most impressive building is the tomb of Bibi Miriam made up of coral blocks and covered with a plaster layer inside with nicely ornamented stucco decoration. The population of Qalhat was cosmopolitan (Agius 1999). Trade was possible due to monsoon winds, and merchant vessels sailed northwards to Makran facilitated by coastal currents (Cleuziou & Tosi 2000). Dates, thoroughbred horses, pearls and frankincense were the most important goods traded.

So far, evidence for the decline of Qalhat as an important trade town is based on historical and archeological studies (e.g. Rougeulle et al. 2014). However, it remains unclear whether human activities (e.g. war) or natural calamities (e.g. earthquake, storm surge or tsunami) can be held responsible. This study aims to give insight into the geological setting on the north-eastern coast of Oman with a focus on the relationship between landforms, sediments and faults. We aim to test the hypothesis if Qalhat was destroyed through an earthquake. The hypothesis is related to the fact that approximately 72 km of the coastal area north of Qalhat is characterised by a set of Pleistocene marine terraces, possibly indicating recent tectonic activity.

Regional Setting

Location and Climate

The Sultanate of Oman is located in the north-east of the Arabian Peninsula and shares borders with the United Arab Emirates to the north-west, Saudi Arabia to the west and Yemen to the south-west. It borders the Gulf of Oman in the north and the Arabian Sea in the east with a coast that stretches over 1700 km from the Strait of Hormuz in the north to the Yemeni border in the south-west. 309.500 km² of the Arabian Peninsula are encompassed by the Sultanate of Oman, between 17° and 26° North and 52° to 60° East. Topographically, the north-eastern part of the Arabian Peninsula is dominated by the Oman Mountains that have a NW-SE extension of about 700 km and a width of up to 120 km, stretching from Musandam in the north-west to Ras Al Hadd in the south-east. The highest peak, Jabal Shams, is 3006 m above sea level (asl).

The Oman Mountains cause orographic rainfall, mostly during the winter months when moist air reaches the area from the Mediterranean. Precipitation is highest in the mountains, where locally annual amounts of up to 250 mm are recorded (Kwarteng, Dorvlo & Vijaya Kumar 2009). Therefore, semi-arid conditions are encountered on the slopes and summits of the Oman Mountains (Al-Charaabi & Al-Yahyai 2013). The areas south of the mountain chain are in the rain shadow and the annual amount of precipitation is less than 50 mm. Rainfall events are sporadic and do not occur every year. Hence the area is characterised as hyper-arid and vast desert regions form here. The interior of Oman is dominated by gravel deserts; sand deserts do also exist.

Plate Tectonic Setting

The study area is located along the passive continental margin of the Arabian Plate. This continental plate borders the Eurasian Plate in the north and north-east, the Indian Plate in the east and the African Plate to the south-west and west (**Figure 1**). The Arabia-India Plate boundary is represented by the Owen Fracture Zone, an 800 km long fault system that accommodates a dextral strike-slip motion between the two plates (Fournier et al. 2011; Rodriguez et al. 2011). To the south, the Owen Fracture Zone is connected to the active spreading axis of the Gulf of Aden and the Red Sea, forming the south-western plate boundary (Hoffmann et al. 2016; Kusky, Robinson & El-Baz 2005). Active spreading of the Red Sea leads to a northward movement of the Arabian Plate. The convergence between the Eurasian and the Arabian Plate resulted in the formation of the Makran accretionary complex in Cenozoic times (Kopp et al. 2000). The Arabian Plate dips 5° north beneath the Makran accretionary wedge (Kopp et al. 2000; Rodgers & Gunatilaka 2003). The subduction of the Arabian Plate along this zone is linked to earthquake activity and earthquake related tsunami in the history of this region (Heidarzadeh et al. 2008). The last earthquake induced tsunami along the shore of Oman was recorded on 28.11.1945 (Hoffmann et al. 2013) The eastern part of the Makran Subduction Zone is seismically more active than the western part which indicates a separation of the eastern and western part of the zone. The reason for the difference in seismicity is unknown (Smith et al. 2013) and hampers the assessment of risk, especially in terms of tsunami generation.

Regional Geology

The geology of the Oman Mountains and adjacent areas is complex. The oldest rock units exposed belong to the crystalline basement of the Arabian Plate, unconformable overlain by various late Proterozoic units. The Paleozoic sequence is fragmentary. Until the Early Permian, sediments were deposited in continental basins and on the continental shelf as the area was part of Gondwana (Glennie 2005). Sedimentation from the Late Permian to Cretaceous resulted in a sequence of carbonates that were deposited on the passive continental margin within the southern Neotethys Ocean (Rabu et al. 1990). The formation of limestone and dolomite terminated with the emplacement of the Samail Ophiolite onto the Arabian Platform (El-Shazly & Coleman 1990; Glennie 2005; Rabu et al. 1990; Searle & Cox 1999; Warren et al. 2005). Changes in plate motion between Africa and Eurasia were accompanied by closing of the Neotethys, leading to the detachment of oceanic lithosphere and therefore initiat-

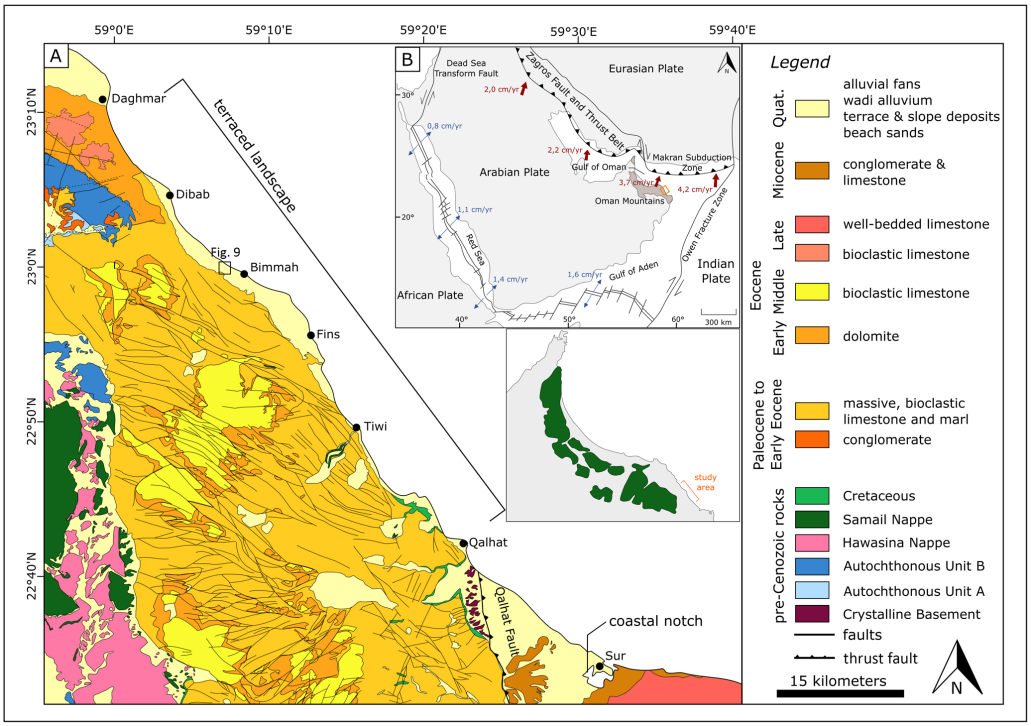

Figure 1: Geology of the study area. **(A)** Study area on the north-eastern coast of Oman with the Qalhat Fault in the south, separating the terraced landscape from the Sur area. Geological map simplified after Al Battashy et al. (2001); El Amin et al. (2005); Le Métour, de Gramont & Villey (1986); Wyns et al. (1992). **(B)** Plate tectonic setting after Hoffmann et al. (2016); Vita-Finzi (2001). **(C)** Extent of the Samail Ophiolite after Searle (2007).

ing the obduction by gravity sliding across the subsiding passive continental margin (Hacker & Gnos 1997; Searle & Cox 1999). The obduction history began with the formation of oceanic lithosphere about 95 Ma ago and was completed by lower Maastrichtian times about 74 Ma (Searle & Cox 1999; Warren et al. 2005). The emplacement of the ophiolite onto the continental margin led to the stacking of deep marine sediments and continental slope deposits. These tectonic nappes were emplaced in front of and underneath the ophiolite (Searle & Cox 1999). The current extent of ophiolitic rocks is shown in **Figure 1**. Shallow marine conditions prevailed during the Late Cretaceous, Paleogene and Neogene carbonates as well as marls were deposited on top of the ophiolite (Wyns et al. 1992). The cumulative thickness of this post-obduction sequence is exceeding 2 000 m. These rocks dominate our study area: the eastern slope of the Selma Plateau.

The landscape's shaping during the Quaternary is a consequence of variable climate and ongoing uplift of the main mountain chain. The amount of precipitation during Pleistocene wet phases was considerably higher and resulted in the karstification of the Mesozoic and Cenozoic limestone formations (Fleitmann et al. 2002; Parker 2010). This is evident through ponors and caves on the surface of the Selma Plateau, as well as by huge wadis with perennial flow that are part of the karst system. Large alluvial fans developed north of the mountains (Abrams & Chadwick 1994).

Alluvial terraces within the mountains and marine terraces along the coast indicate ongoing uplift (Kusky, Robinson & El-Baz 2005). Hoffmann, Rupprechter & Mayrhofer (2013) demonstrated that the crustal deformation is not uniform and that especially the coastal area between Daghmar in the north and Qalhat in the south is characterised by uplift, geomorphological expressed by a flight of marine terraces. Beachrock deposits on the terrace surfaces provide evidence for their marine origin (Falkenroth, Schneider & Hoffmann 2019). Moraetis et al. (2018) studied these terraces and uplifted coastal notches to generate an age model and calculate uplift rates. ^{14}C dating of six samples led to an average uplift rate ranging from 0.9 ± 0.1 to 6.7 ± 0.9 mm/a indicating differential uplift along the coast (Moraetis et al. 2018). The two lowermost terraces were sampled, leading to a maximum age of 48020 ± 2030 a cal BP at an elevation of approximately 46 m asl (Moraetis et al. 2018). However, there are terrace levels up to elevations of 500 m asl and at least 12 terrace levels in total (Falkenroth, Schneider & Hoffmann 2019).

Currently the causative mechanism for the observed uplift is not convincingly solved. Models described by Rodgers & Gunatilaka (2003), Kusky, Robinson & El-Baz (2005), Yuan, Kusky & Rajendran (2016) and Moraetis et al. (2018) are partly contradicting but the main process for differential uplift is seen in lithospheric flexure in combination with forebulge migration as a consequence of the subduction process in the Makran Subduction Zone. Kusky, Robinson & El-Baz (2005) conclude that the intraplate deformation is the reason for numerous faults dissecting the landscape and that at least some of those faults may indicate neotectonic movements. The most prominent structural element within our study area is the Qalhat Fault. This N-S striking fault (**Figure 1**) separates the uplifting area in the north-west from the stable area in the south-east. The Qalhat Fault is a normal fault that developed during Late Cretaceous to Early Eocene extensional stages which followed ophiolite obduction

(Fournier et al. 2006; Gray 2000; Wyns et al. 1992). During a Miocene compressional stage, related to the collision process leading to the Zagros Mountains (Fournier et al. 2006), the fault was reactivated as an east-verging reverse fault, thrusting older deposits in the form of Maastrichtian and Early to Middle Eocene rocks over Miocene deposits across a fault plane dipping 60° towards the West (Wyns et al. 1992).

Methods – Structural Analyses

Faults were mapped in the field and complemented by digital analyses of a digital elevation model (DEM), including lineament and drainage system investigations (**Figure 2**), which both are commonly used for fault identification (Burbank & Anderson 2011; Gorshkov et al. 2000; Gupta 2013; Jordan 2003; Koike, Nagano & Kawaba 1998). A DEM for the digital analyses was provided by the German Aerospace Center that has been performing the TanDEM-X mission since 2010 in order to produce a high resolution DEM covering the whole earth (Zink et al. 2006; Zink, Bartusch & Miller 2011).

The DEM for the Oman region has a resolution of 12.37 m with an uncertainty in height between two DEM pixels of two meters (Wessel 2016). The standard DEM has a pixel spacing of 0.4 arc-seconds, which accords between 12.37 m – 12.33 m from the equator to the poles (Wessel 2016). The TanDEM-X DEMs therefore have big advantages over the established digital elevation data with resolutions of 30 meters (ASTER, SRTM) (Bartusch et al. 2009; Smith & Pain 2009; Wessel 2016).

Field Work

Field work was conducted for two weeks in March 2017 in the area between Dibab and Qalhat. As the northern part of the study area is hard to access, this area was analysed by remote sensing only. For analysing the tectonic situation in the investigated area, numerous faults were identified in the Eocene limestone formations. Most of them were exposed quite well so that fault surfaces could be measured with a geological compass.

Figure 3 shows three examples of exposed faults. Most of the identified faults appeared like the faults shown in **Figure 3A**; large-scale faults like the one in **Figure 3C** were investigated in the walls of wadi channels.

Lineament Analysis

Hobbs (1904) was the first scientist who used the term lineament by defining it as a "significant line of landscape which reveals the hidden architecture of rock basement". Lineament is now a widely used term and often includes different matters depending on the focus of study. The term can be used for geological features like faults, shear zones, rift valleys, fracture traces or for linear characteristics due to lithological layering. It also can describe geomorphological features like the alignment of streams and valleys, topographic elements like ridges or even linear vegetation formations (Gupta 2013). For the purpose of this study, lineaments are defined as prominent, linear structures of non-anthropogenic origin in the landscape that can be identified clearly in the DEM. These lineaments can further be interpreted as zones of rock weakness or, respectively, fault zones, leading to increased erosion and therefore acting as a helpful tool for the identification of fault zones (Burbank & Anderson 2011; Jordan et al. 2005).

For lineament analysis the software ArcMap10.3.1 was used. It provides 8 relief shading models for illumination angles at intervals of 45° (**Figure 2**).

Drainage System Analyses

The drainage network that was extracted from the DEM shows a dendritic pattern following slope and topography (**Figure 2**). This given drainage system was examined in terms of drainage anomalies, which describe any kind of local deviation from the original dendritic drainage pattern (Huggett 2007; Ramasamy et al. 2011). These deviations are defined as deflected channels or compressed meanders (**Figure 2**) and their analyses is a common method in geomorphological studies as the drainage system is likely controlled by neo-tectonic deformation (Bhosle et al. 2009; Estrada 2015; Ramasamy et al. 2011). Deflected drainage may be caused by lineaments crossing the stream and deflecting it, whereas compressed meanders may also indicate a vertical component (Deffontaines et al. 1997; Ramasamy et al. 2011). The drainage system is not only controlled by structural elements, but also by the terrace morphology. Consequently, the analysis itself was conducted non-automatically to distinguish between tectonically and morphological influenced anomalies as well as lineaments resulting from anthropogenic features.

Results – Evidence for Neo-Tectonic Activity

The vegetation cover is sparse within our study area due to the semiarid climatic conditions. The rocks are therefore exposed and our remote sensing approach was successful. The faults detected during field work and lineaments identified in the digital analyses are compiled in a structural map (**Figure 3**). In total, 147 lineaments are detected along the coastline. The upper terraces in the study area are mostly erosional with Eocene bedrock exposed. Quaternary sediments are rare as only lag deposits in form of cemented beach deposits are identified. The lower three terraces are depositional and the Quaternary terrace fill has different facies representing beach deposits, alluvial fans, deltas and coral reefs. These deposits are partly cemented. Most of the lineaments are identified in the upper, erosional terraces and therefore constraints on the timing of potential faulting must remain imprecise. The rose diagram in **Figure 2** shows the dominant strike direction as NW-SE with a slight tendency towards the west. Additionally, a small number of lineaments strike in other directions. Examples of faults in the field, affecting the Eocene bedrock are shown in **Figure 3A, 3B** and **3C**. The dominant fault orientation is WNW-ESE with a tendency towards a NW-SE striking fault direction (rose diagram, **Figure 3**), hence the lineaments are interpreted as faults. The faults are parallel to the mountain front in the Oman Mountains.

The WNW-ESE striking faults are not single fault planes, but rather form zones of complex deformation. For matters of simplification we describe them as fault zones. The marine terraces along the coast are the record for coastal

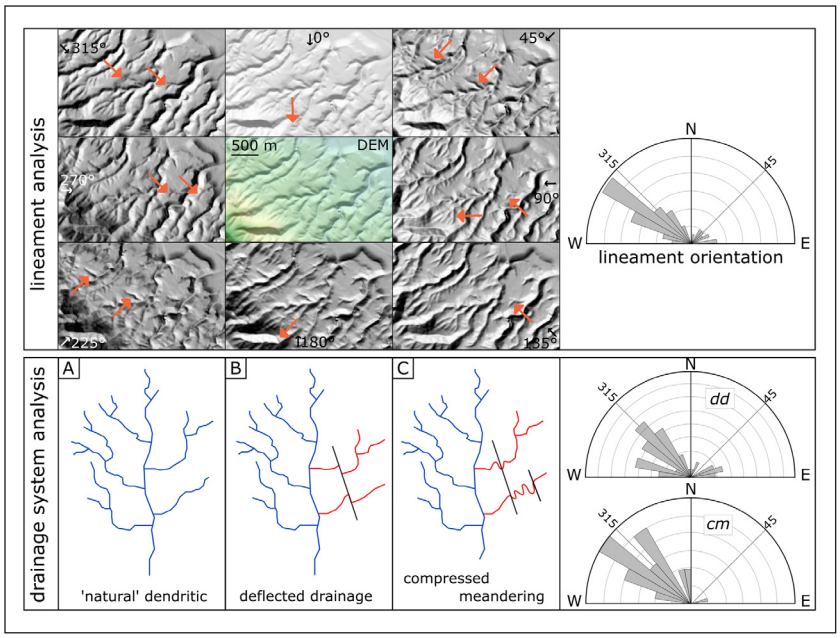

Figure 2: Lineament and drainage system analyses. Lineament analysis (top): The digital elevation model in the center, surrounded by relief shading models for eight different illumination angles which are noted for each model. Orange arrows point perpendicular to lineaments. The rose diagram shows a dominant lineament orientation roughly striking NW-SE. Drainage system analysis (bottom): The natural dendritic drainage pattern **(A)** and the most common drainage anomalies resulting by fault zones: deflected drainage **(B)** and compressed meandering **(C)**. The rose diagrams show the directions of the detected drainage anomalies (dd = deflected drainage; cm = compressed meandering).

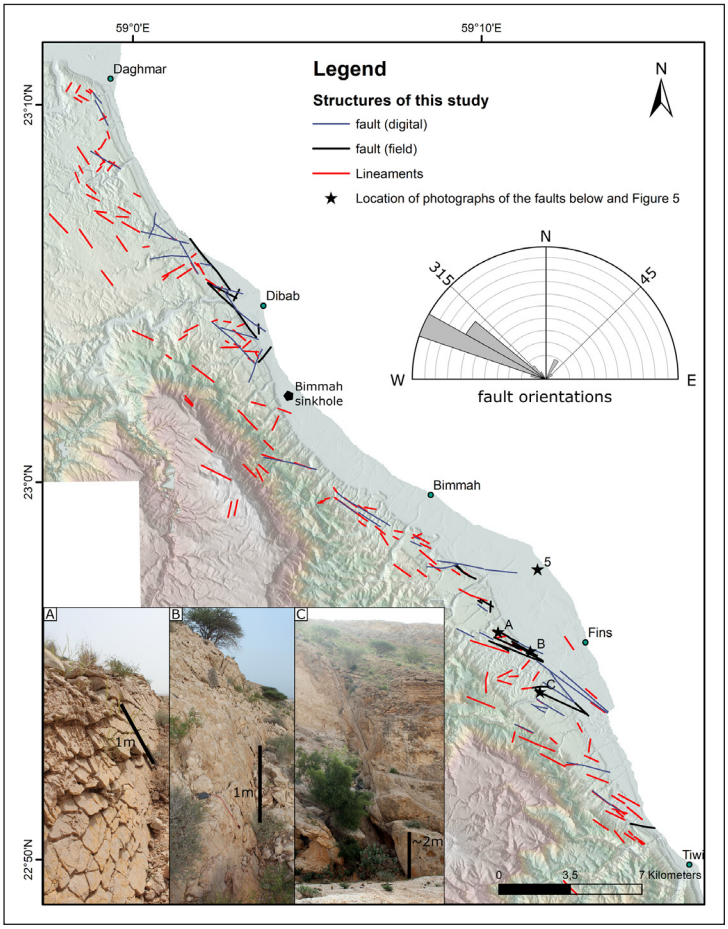

Figure 3: Structure map of the study area. Structure map of the area between Daghmar and Tiwi, showing both the digital and field results and a rose diagram of all detected faults. **(A), (B), (C):** Examples for faults in different dimensions detected in the field, the location of each fault is noted on the map. The location of the photography in Figure 5 is located as well.

uplift in the Pleistocene as outlined in detail by Moraetis et al. (2018) (**Figure 4**). The terraces have abrupt elevation changes along the fault zones which implies that the faulting occurred after the formation of the marine terraces. The rose diagrams in **Figure 4** show the orientation of the terrace scarps and the detected faults cutting through them. The orientation differs, indicating that the terraces formed by uplift of abrasion platforms and not by faulting. The fault zones define the boundaries of five different tectonic blocks. **Figure 5A** shows the location of the fault zones, which we labelled from north to south the Dibab Fault Zone, Bimmah Fault Zone, Fins Fault Zone and Tiwi

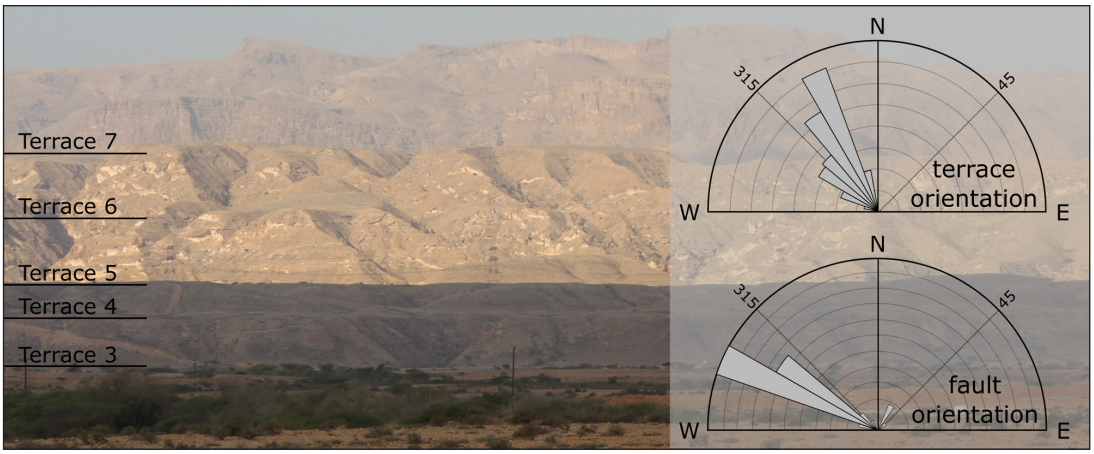

Figure 4: Terraces and rose diagrams of the detected faults and terraces. The dissenting directions confirm that the terraces do not represent fault surfaces and are merely of conventional marine terrace origin. The location of the photography is marked in Figure 4.

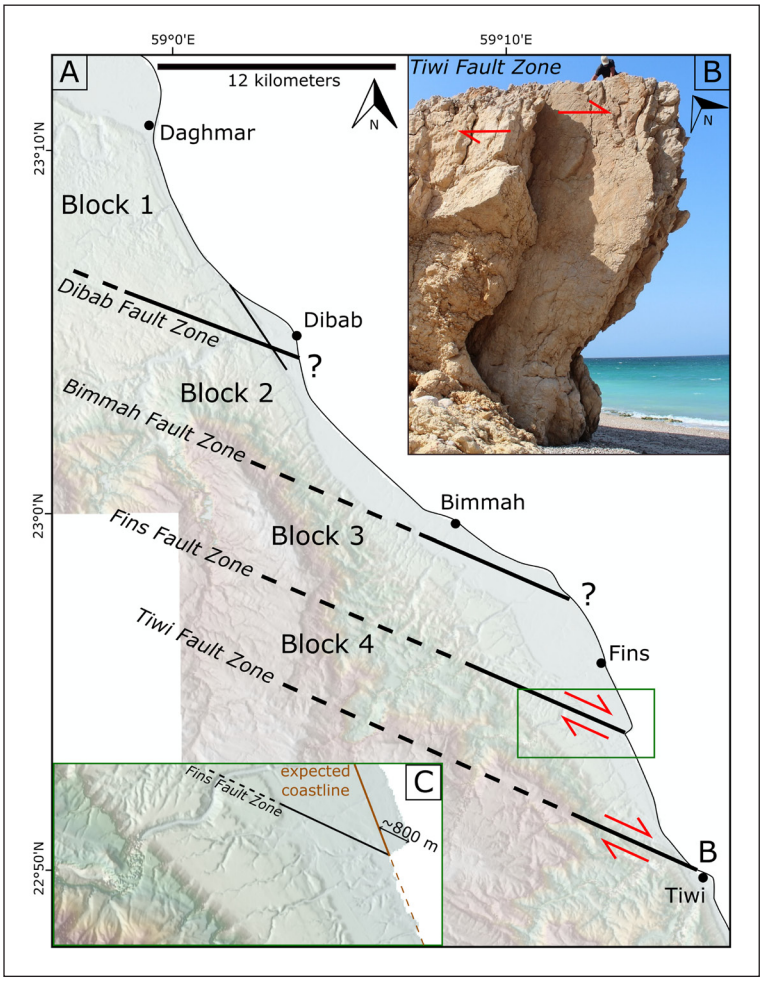

Figure 5: Model for the displacement of tectonic blocks relative to each other. The topography is displayed in the background, as it also supports this theory. An escarpment follows the course of the southernmost Tiwi Fault Zone. This zone also comprises the fault proving evidence for movement of the blocks relative to each other by slickensides on the fault surface shown in **(B)**. These slickensides indicate a dextral movement. **(C)** The coastline south of Fins indicates a dextral movement direction as well and an offset of approximately 800 meters.

Fault Zone. Movement directions are difficult to assess for the northernmost fault zones around Dibab and Bimmah. Field evidence for a dextral movement in the southern Tiwi Fault Zone is represented by slickensides on the fault plane (**Figure 5B**). The fault plane is orientated 0/85 while the slickensides dip between 10° and 15°, indicating oblique strike slip movement. Relative movement along the Fins Fault Zone is evident by a displacement of the coastline with an offset of approximately 800 meters (**Figure 5C**). Age constraints and related movement rates are vague, as the Eocene bedrock is offset. The terrace morphology ends abruptly south of the Qalhat Fault. The Qalhat Fault therefore is seen as the major structural element that accommodates relative crustal movement. As no more terraces are observed we regard the area south of Qalhat as stable whereas uplift is observed towards the north.

A prominent terrace, elevated approximately 30 m asl in the northern part of the study area is correlated to MIS 3 by Moraetis et al. (2018). Here, the terrace fill shows offsets along fault planes. **Figure 6A** illustrates the major fault surface displacing the conglomeratic deltaic terrace deposits. This surface strikes WNW-ESE dipping 82° towards the SSW. In the upper part of this outcrop, a second fault approximately perpendicular to the major fault dissects the large fault surface (**Figure 6B**). This indicates multiple successive tectonic activities with different fault generations. The faulting must be younger than the terraces deposits and must have taken place after MIS 3 (e.g. <50.000 years). Small-scale fractures and fissures were mapped on the lowermost terrace and indicate neotectonic activity as well as they strike in the major fault direction WNW-ESE (**Figure 6C** and **D**).

The final observation with regard to recent deformation of the surface is related to the drainage pattern. Drainage anomalies in the form of deflected drainage and compressed meandering are observed (**Figure 2**). The rose diagrams in **Figure 2** show the orientation of the detected drainage anomalies. The main direction of flow influence is striking NW-SE, parallel to the lineaments. The drainage pattern on the terraces is a comparatively young element in the landscape that can only have formed after terrace emergence.

Discussion

The coastal morphology with a staircase of marine terraces proves differential movement of the lithosphere. The tectonic origin of the terraces as suggested by Yuan, Kusky & Rajendran (2016) stating that the terrace scarps represent fault surfaces is in disagreement with our data as the tectonic structures appear in WNW-ESE striking directions while the terrace scarps are orientated NNW-SSE. The terraces formed rather as abrasion platforms as outlined in detail by Falkenroth, Schneider & Hoffmann (2019). The marine terraces stretch along 72 km of the coast and terminate near the ancient town of Qalhat. Elevation differences between paleo-shorelines along the coast are considerable. The lagoon in Sur (**Figure 1**) located south of Qalhat is characterised by coastal notches

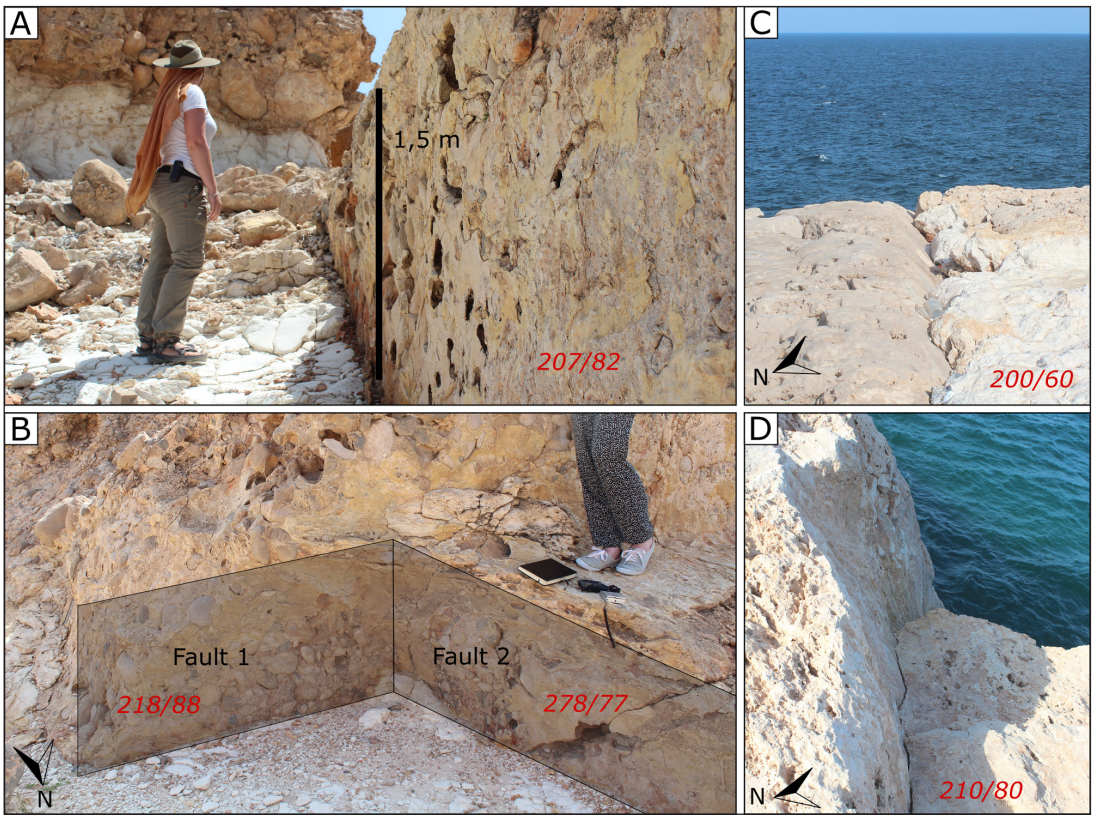

Figure 6: Faults and fissures along the coast. **(A)** and **(B)** Faults in the area around Dibab proving the youngest tectonic activity (Location: 23°04'N/59°02'E). The major fault (fault 1 and fault surface in (A)) is displaced by a younger fault (fault 2) by approximately 2 meters. The fault surfaces in (B) indicate two fault generations. Measurements are noted in red. **(C)** and **(D):** Small-scale fissures and fractures on the lowermost terrace near the coast, striking in the major fault direction and therefore indicating recent tectonic activity. These small-scale fractures can be found south of Tiwi (approximate location: 22°47'N/59°16'E).

along its rocky shores. These bio-erosional notches are in elevations of approximately 4 m asl, and are dated to 80 ± 3 ka by Mauz et al. (2015). One of the terraces north of Qalhat correlated to MIS 3 by Moraetis et al. (2018), is elevated approximately 30 m asl.

The termination of the uplifting coastal area coincides with the Qalhat Fault. The fault extends over more than 20 km with a maximum vertical displacement of approximately 5 km (Ali, Al Bahri & Al Harthy 2016; Wyns et al. 1992). Our field observations, e.g. neotectonic deformation of the lower and younger terraces fill deposits, as well as deflected drainages, indicate rather young deformation and therefore support the possibility of fault activity in the fifteenth century as discussed by Kusky, Robinson & El-Baz (2005), Moraetis et al. (2018), Wyns et al. (1992). However, our age constraints remain vague.

The dominant direction of the faults is WNW-ESE indicating an interrelation with the Makran Subduction Zone that strikes parallel. Therefore, the most plausible interpretation of the geomorphological situation is the development of a flexural, lithospheric bulge due to the subduction process as already identified by Rodgers & Gunatilaka (2003) or Yuan, Kusky & Rajendran (2016). However, the observed uplift is not uniform. The regional fault system as mapped on a scale of 1:100000 by Le Métour, de Gramont & Villey (1986) and Wyns et al. (1992) shows a radial pattern in the southern part (**Figures 1A, 7**) whereas some faults in the northern part are trending parallel to the subduction zone. The fault pattern indicates two uplift centers (**Figure 7**). We observe differential movement of the terraces along the coast as the elevation of all terrace surfaces increases towards the SSE (**Figure 8**) induced by higher uplift rates towards the south as already described by Moraetis et al. (2018). Radial fault patterns as documented for our study area (Wyns et al. 1992) are known to develop in updoming environments and are predominantly described for salt diapirs (Carruthers et al. 2013; Stewart 2006). Withjack & Scheiner (1982) conducted several clay model experiments in order to identify different fault patterns for updoming environments in general, and conclude that salt diapirism as well as the uplift of basement rocks create folded or faulted overlying sediments.

The termination of the marine terraces on the Qalhat Fault coincides with the distribution of the Samail Ophiolite underlying the Late Cretaceous, Paleogene and Neogene limestone formations. Serpentinisation is a well-known process in ophiolite alteration (Searle & Cox 1999; Streit, Kelemen & Eiler 2012) and several studies prove ongoing low-temperature serpentinisation in our study area (Kelemen & Matter 2008; Mervine et al. 2014). Geochemical reactions involved with the serpentinisation of peridotites induce a volume increase and density

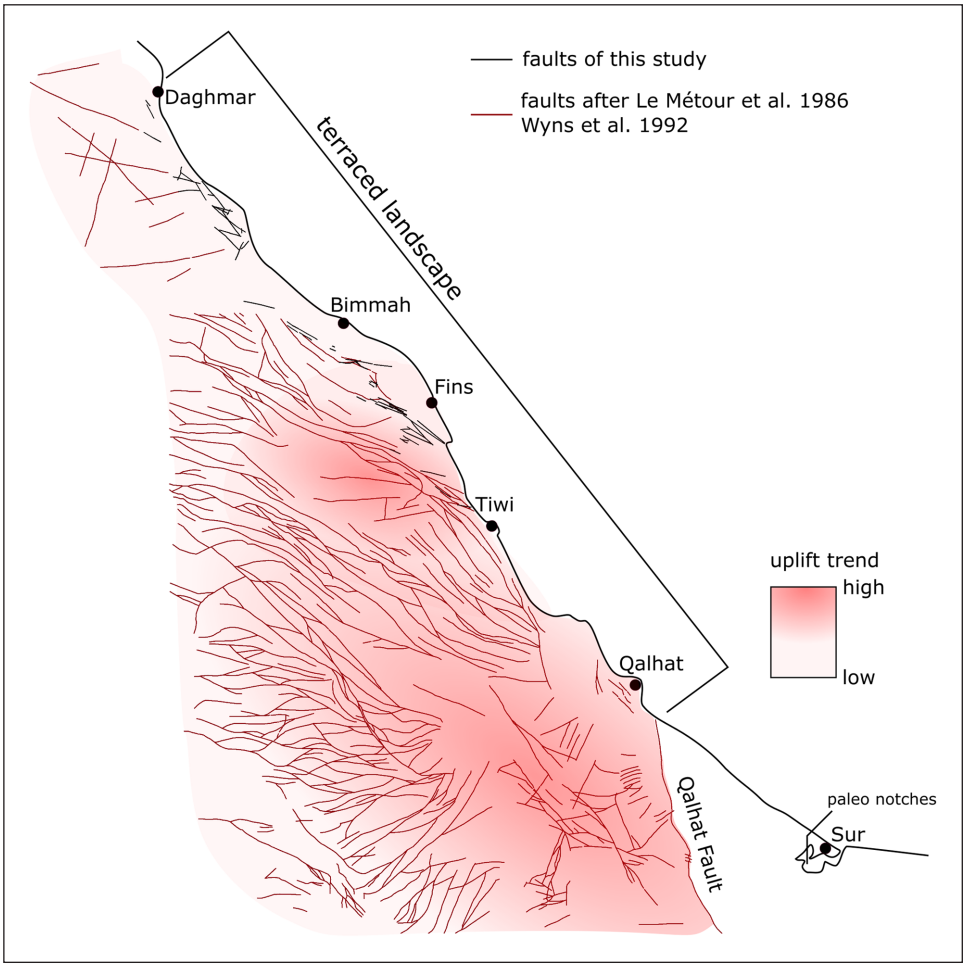

Figure 7: Radial fault pattern in the study area. The radial fault pattern derived by the geological maps after Le Métour, de Gramont & Villey (1986) and Wyns et al. (1992) indicate locally higher uplift rates induced by dome-like uprising of serpentinite.

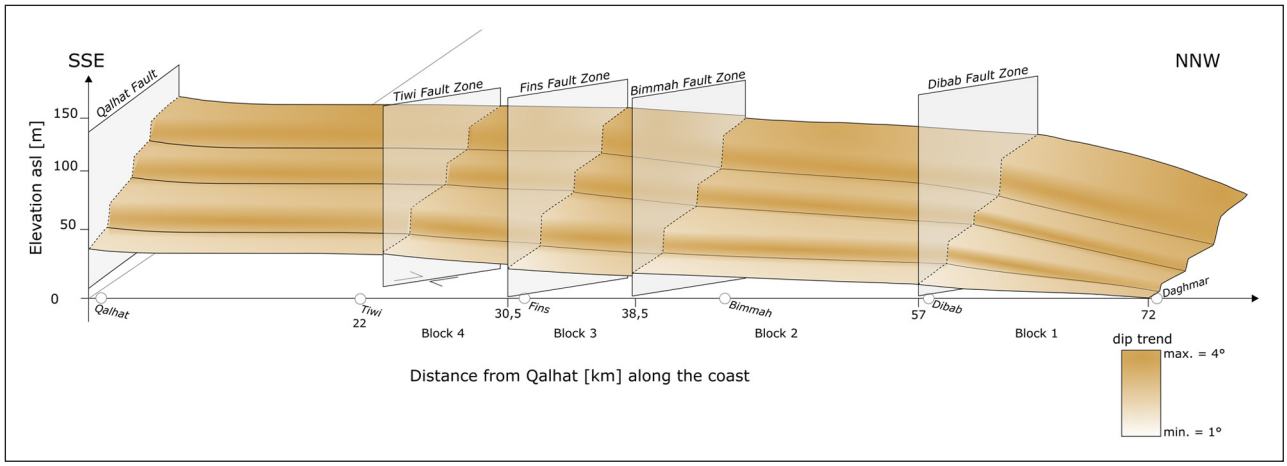

Figure 8: Model for the terraced landscape from Daghmar in the NNW to Qalhat in the SSE. Four fault zones, the Dibab Fault Zone, Bimmah Fault Zone, Fins Fault Zone and Tiwi Fault Zone, divide the terraced area in four separated blocks. The Qalhat Fault represents the southern termination of this landscape, the block south of Qalhat is stable.

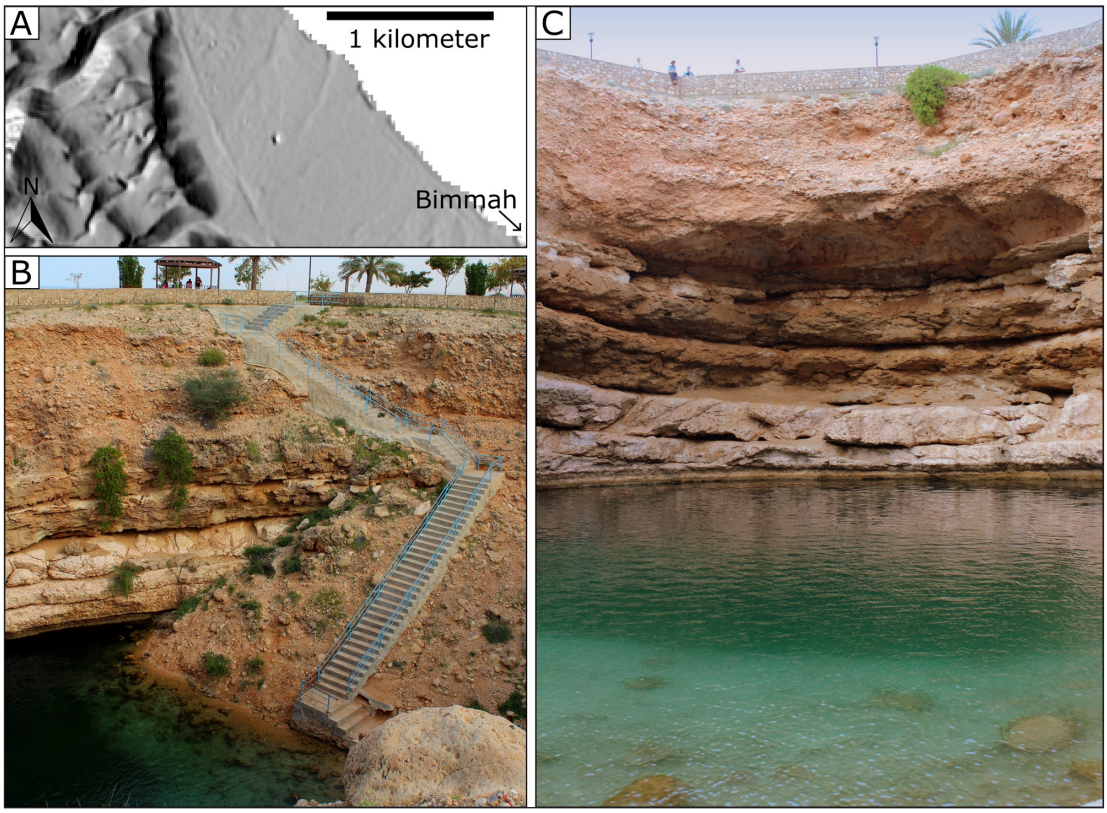

Figure 9: Example of karstification. The Bimmah sinkhole. **(A)** location of the sinkhole (dot in the centre) as depicted in the digital elevation model. **(B)** and **(C)** the stratigraphy exposed in the sinkhole shows Eocene limestone, overlain by deltaic Pleistocene deposits.

decrease (Malvoisin 2015). A complete serpentinisation of the peridotitic rocks may lead to a volume expansion calculated as 44% (Schuiling 2011) or even 50% (Jamtveit & Austrheim 2010). Serpentine diapirism including substantial uplift as a consequence is described for Cyprus (Poole & Robertson 1991) and may be of significance in our study area as well. The geological setting is very similar as the Troodos Complex (Cyprus) is a remnant of the Tethys oceanic crust (Grebby et al 2010), as is the Samail Ophiolite of Oman. Both are emplaced over passive continental margins in relation to the closing Neotethys (Dilek & Robinson 2003).

Another process that needs to be considered is isostatically driven vertical uplift. Coastal uplift as isostatic response to karstification is seen as an important process along the coast of north Florida (Adams, Opdyke & Jaeger 2010; Opdyke et al. 1984; Woo et al. 2017). Our study area is characterised by intense karstification resulting in an open karst system that includes the large wadis. Common features along the coast are sink holes (**Figure 9**), springs and caves (Hoffmann et al. 2016; Rajendran & Nasir 2014).

Intraplate earthquakes are known for the area under study (El-Hussain et al. 2012). Musson (2009) reports earthquakes near Qalhat in the years 1971 and 1984 and

speculates about an active seismic zone in the vicinity. The tentatively proposed recent (e.g. 500 years ago) activity of the Qalhat Fault is supported by archaeological evidence within the ancient city of Qalhat. Detailed archeological studies of the ruins of Qalhat show that citizens were aware of earthquake potential. Rougeulle (2017) reports on the great mosque building in the city centre that collapsed in an abnormal asymmetrical way. Walls of this building were supported by retaining walls (Rougeulle 2017). Both findings, as well as the historical evidence that the town of Qalhat was under reconstruction when the Portuguese destroyed it in the early 16th century, are interpreted as the evidence for earthquake activity along the Qalhat Fault (Rouguelle 2017).

Conclusion

Recent deformation of the lithosphere within our study area is seen in faults cutting through terrace fill deposits, in the geomorphology of the terraced landscape and in deflected drainage patterns. Field observations combined with high resolution digital structural analyses including lineament and drainage system investigations of the terraced landscape, show that the study area is dissected by faults. The orientations of terrace and fault scarps clarify that the terraces are not of tectonic origin. A radial fault pattern of the terraced area is interpreted as locally intensified uplift that may be caused by serpentinite diapirism. The termination of the terraces south of Qalhat indicates that the Qalhat Fault represents the boundary between an uplifting block in the north and a stable block in the south. The neotectonic deformation patterns described, e.g. evidence for a dextral movement along the Tiwi Fault Zone, are 20 km to the NW of Qalhat itself.

However, as the coastal terraces terminate on the Qalhat Fault, tectonic activity along the fault 500 years ago is possible and the hypothesis that an earthquake along this fault resulted in the destruction of the ancient town of Qalhat is plausible. Archeological and historical studies support this assumption. We recommend to carry out structural analysis on the Qalhat Fault itself to assess the risk.

Our results are relevant as urbanisation is expanding significantly within the study area. The most critical infrastructure installed to date is a gas liquefaction plant, located right on the Qalhat Fault.

Acknowledgements

This paper is a contribution to IGCP project 639 "Sea level changes from minutes to millennia". We gratefully thank the German Aerospace Center (DLR) for the digital elevation data that was provided by DLR's TerraSAR-X/TanDEM-X satellite mission. The authors would like to thank Stefani Clark for the final language check. Additionally, help from Sophia Blech during fieldwork is gratefully acknowledged. The thorough by reviews by Rich Briggs and an anonymous reviewer helped tremendously to improve the quality of the manuscript. And finally, the excellent fieldtrip logisitics supplied by Golden Highlands Oman made a big difference.

Funding Information

Financial support by The Research Council Oman (TRC-grant ORG GUtech EBR 10 013; ORG-EBR-10-006) and funding of the Deutsche Forschungsgemeinschaft (DFG, German Research Foundation) (HO2550/11-1) is gratefully acknowledged.

Competing Interests

The authors have no competing interests to declare.

Author Contributions

AE carried out the fieldwork and prepared the figures and text. GH carried out fieldwork and contributed to the text. MF supported the fieldwork and contributed to the text. MK and SKA supported the fieldwork.

References

Abrams, MJ and **Chadwick, OH.** 1994. Tectonic and climatic implications of alluvial fan sequences along the Batinah coast, Oman. *Journal of the Geological Society*, 151(1): 51–58. DOI: https://doi.org/10.1144/gsjgs.151.1.0051

Adams, PN, Opdyke, ND and **Jaeger, JM.** 2010. Isostatic uplift driven by karstification and sea-level oscillation. Modeling landscape evolution in north Florida. *Geology*, 38(6): 531–534. DOI: https://doi.org/10.1130/G30592.1

Agius, D. 1999. Medieval Qalhat: travellers, dhows and stone anchors in south-east Oman. In: Ray, HP (ed.), *Archaeology of Seafaring*, 173–220. Delhi: Pragati Publications.

Al Battashy, M, Hauser, M, Immenhauser, A, Moser, L, Peters, T and **Al Rajhi, A.** 2001. Geological Map – Sur/Al Ashkharah 1: 100.000. Sheet NF 40-8F and Sheet NF 40-12C. Muscat: Ministry of Commerce and Industry, Sultanate of Oman.

Al-Charaabi, Y and **Al-Yahyai, S.** 2013. Projection of future changes in rainfall and temperature patterns in Oman. *Journal of Earth Science & Climate Change*, 4(5): 154–161. DOI: https://doi.org/10.4172/2157-7617.1000154

Ali, M, Al Bahri, QA and **Al Harthy, A.** 2016. Gravity Experiment in Oman for Exposing a Basin. *Bahria University Research Journal of Earth Sciences*, 1: 24–27.

Bartusch, M, Hajnsek, I, Janoth, J, Marschner, C, Miller, D, Moreira, A, Sparwasser, N and **Zink, M.** 2009. TanDEM-X – Die Erde in drei Dimensionen. Bonn: Deutsches Zentrum für Luft- und Raumfahrt e.V.

Bhacker, MR and **Bhacker, B.** 2004. Qalhāt in Arabian history: context and chronicles. *Journal of Oman Studies*, 13: 11–55.

Bhosle, B, Parkash, B, Awasthi, AK and **Pati, P.** 2009. Use of digital elevation models and drainage patterns for locating active faults in the Upper Gangetic Plain, India. *International Journal of Remote Sensing*, 30(3): 673–691. DOI: https://doi.org/10.1080/01431160802392604

Boivin, N and **Fuller, DQ.** 2009. Shell middens, ships and seeds: Exploring coastal subsistence, maritime trade and the dispersal of domesticates in and around the ancient Arabian Peninsula. *Journal of World Prehistory*, 22(2): 113–180. DOI: https://doi.org/10.1007/s10963-009-9018-2

Burbank, DW and **Anderson, RS.** 2011. *Tectonic geomorphology*. Oxford: John Wiley & Sons. DOI: https://doi.org/10.1002/9781444345063

Carruthers, D, Cartwright, J, Jackson, MPA and **Schutjens, P.** 2013. Origin and timing of layer-bound radial faulting around North Sea salt stocks. New insights into the evolving stress state around rising diapirs. *Marine and Petroleum Geology*, 48: 130–148. DOI: https://doi.org/10.1016/j.marpetgeo.2013.08.001

Cleuziou, S and **Tosi, M.** 2000. Ras al Jinz and the Prehistoric coastal cultures of the Jalan. *Journal of Oman Studies*, 11: 19–74.

Deffontaines, B, Lacombe, O, Angelier, J, Chu, HT, Mouthereau, F, Lee, CT, Deramond, J, Lee, JF, Yu, MS and **Liew, PM.** 1997. Quaternary transfer faulting in the Taiwan Foothills. Evidence from a multisource approach. *Tectonophysics*, 274(1–3): 61–82. DOI: https://doi.org/10.1016/S0040-1951(96)00298-3

Dilek, Y and **Robinson, PT.** (eds.) 2003. *Ophiolites in earth history*. London: Geological Society of London. DOI: https://doi.org/10.1144/GSL.SP.2003.218.01.01

El Amin, O, Peters, T, Blechschmidt, I, Al-Battashi, M, Al-Khumasani, N and **Al-Towaya, A.** 2005. Geological Map – Ibra 1: 100.000. Sheet NF 40-8A. Muscat: Ministry of Commerce and Industry, Sultanate of Oman.

El-Hussain, I, Deif, A, Al-Jabri, K, Toksoz, N, El-Hady, S, Al-Hashmi, S, Al-Toubi, K, Al-Shijbi, Y, Al-Saifi, M and **Kuleli, S.** 2012. Probabilistic seismic hazard maps for the sultanate of Oman. *Natural hazards*, 64(1): 173–210. DOI: https://doi.org/10.1007/s11069-012-0232-3

El-Shazly, AK and **Coleman, RG.** 1990. Metamorphism in the Oman Mountains in relation to the Semail ophiolite emplacement. In: Robertson, AHF, Searle, MP and Ries, AC (eds.), *The Geology and Tectonics of the Oman Region*, 473–493. London: Geological Society of London Special Publications 49. DOI: https://doi.org/10.1144/GSL.SP.1992.049.01.30

Estrada, B. 2015. Application of drainage analysis to infer "hidden" regional or local tectonic deformation. *Bulletin of Engineering Geology and the Environment*, 74(2): 493–506. DOI: https://doi.org/10.1007/s10064-014-0628-2

Falkenroth, M, Schneider, B and **Hoffmann, G.** 2019. Beachrock as sea-level indicator–a case study at the coastline of Oman (Indian Ocean). *Quaternary Science Reviews*, 206: 81–98. DOI: https://doi.org/10.1016/j.quascirev.2019.01.003

Fleitmann, D, Burns, SJ, Neff, U, Mangini, A and **Matter, A.** 2002. Changing moisture sources over the last 330,000 years in Northern Oman from fluid-inclusion evidence in speleothems. *Quaternary Research*, 60(2): 223–232. DOI: https://doi.org/10.1016/S0033-5894(03)00086-3

Fournier, M, Chamot-Rooke, N, Rodriguez, M, Huchon, P, Petit, C, Beslier, MO and **Zaragosi, S.** 2011. Owen fracture zone: the Arabia–India plate boundary unveiled. *Earth and Planetary Science Letters*, 302(1–2): 247–252. DOI: https://doi.org/10.1016/j.epsl.2010.12.027

Fournier, M, Lepvrier, C, Razin, P and **Jolivet, L.** 2006. Late Cretaceous to Paleogene Post-obduction extension and subsequent Neogene compression in Oman Mountains. *GeoArabia*, 11(4): 17–40.

Fritz, HM, Blount, CD, Albusaidi, FB and **Al-Harthy, AHM.** 2010. Cyclone Gonu storm surge in Oman. *Estuarine, Coastal and Shelf Science*, 86(1): 102–106. DOI: https://doi.org/10.1016/j.crte.2009.03.005

Giraud, J. 2009. The evolution of settlement patterns in the eastern Oman from the Neolithic to the Early Bronze Age (6000–2000 BC). *Comptes Rendus Geoscience*, 341(8–9): 739–749. DOI: https://doi.org/10.1016/j.crte.2009.03.005

Glennie, KW. 2005. *The geology of the Oman Mountains. An outline of their origin*. 2nd ed. Beaconsfield: Scientific Press Bucks.

Gorshkov, AI, Kuznetsov, IV, Panza, GF and **Soloviev, AA.** 2000. Identification of future earthquake sources in the Carpatho-Balkan orogenic belt using morphostructural criteria. *Pure and Applied Geophysics*, 157: 79–95. DOI: https://doi.org/10.1007/PL00001101

Gray, DR. 2000. A new structural profile along the Muscat-Ibra transect, Oman Implications for emplacement of the Samail ophiolite. In: Dilek, Y, Moores, EM, Elthon, D and Nicolas, A (eds.), *Ophiolites and Oceanic Crust: New Insights From Field Studies and the Ocean Drilling Program*, 513–522. Boulder, Colorado: Geological Society of America GSA Special Papers 349. DOI: https://doi.org/10.1130/0-8137-2349-3.513

Grebby, S, Cunningham, D, Naden, J and **Tansey, K.** 2010. Lithological mapping of the Troodos ophiolite, Cyprus, using airborne LiDAR topographic data. *Remote Sensing of Environment*, 114(4): 713–724. DOI: https://doi.org/10.1016/j.rse.2009.11.006

Gupta, RP. 2013. *Remote sensing geology*. Berlin: Springer Science & Business Media.

Hacker, BR and **Gnos, E.** 1997. The conundrum of Samail. Explaining the metamorphic history. *Tectonophysics*, 279(1): 215–226. DOI: https://doi.org/10.1016/S0040-1951(97)00114-5

Heidarzadeh, M, Pirooz, MD, Zaker, NH, Yalciner, AC, Mokhtari, M and **Esmaeily, A.** 2008. Historical tsunami in the Makran Subduction Zone off the southern coasts of Iran and Pakistan and results of numerical modeling. *Ocean Engineering*, 35(8): 774–786. DOI: https://doi.org/10.1016/j.oceaneng.2008.01.017

Hobbs, WH. 1904. Lineaments of the Atlantic border region. *Bulletin of the Geological Society of America*, 15(1): 483–506. DOI: https://doi.org/10.1130/GSAB-15-483

Hoffmann, G, Meschede, M, Zacke, A and **Al Kindi, M.** 2016. *Field Guide to the Geology of Northeastern Oman*. Stuttgart: Borntraeger Science Publishers (Geological Field Guides, 110).

Hoffmann, G, Reicherter, K, Wiatr, T, Grützner, C and **Rausch, T.** 2013. Block and boulder accumulations along the coastline between Fins and Sur (Sultanate of Oman): tsunamigenic remains? *Natural Hazards*, 65(1): 851–873. DOI: https://doi.org/10.1007/s11069-012-0399-7

Hoffmann, G, Rupprechter, M and **Mayrhofer, C.** 2013. Review of the long-term coastal evolution of North Oman-subsidence versus uplift [Review der langfristigen Küstenentwicklung Nordomans-Senkung und Hebung]. *Zeitschrift der Deutschen Gesellschaft für Geowissenschaften*, 164(2): 237–252. DOI: https://doi.org/10.1127/1860-1804/2013/0002

Hourani, GF and **Carswell, J.** 1995. *Arab seafaring in the Indian Ocean in ancient and early medieval times*. Princeton, New Jersey: Princeton University Press.

Huggett, R. 2007. *Fundamentals of Geomorphology*. London: Routledge. DOI: https://doi.org/10.4324/9780203947111

Ibrahim, M and **El Mahi, AT.** 2000. A Survey between Quriyat and Sur in the Sultanate of Oman (1997). *Proceedings of the seminar for Arabian Studies*, 30: 119–136.

Jamtveit, B and **Austrheim, H.** 2010. Metamorphism: the role of fluids. *Elements*, 6(3): 153–158. DOI: https://doi.org/10.2113/gselements.6.3.153

Jordan, G. 2003. Morphometric analysis and tectonic interpretation of digital terrain data: a case study. *Earth Surface Processes and Landforms*, 28(8): 807–822. DOI: https://doi.org/10.1002/esp.469

Jordan, G, Meijninger, BML, van Hinsbergen, DJJ, Meulenkamp, JE and **van Dijk, PM.** 2005. Extraction of morphotectonic features from DEMs. Development and applications for study areas in Hungary and NW Greece. *International Journal of Applied Earth Observation and Geoinformation*, 7(3): 163–182. DOI: https://doi.org/10.1016/j.jag.2005.03.003

Kelemen, PB and **Matter, JM.** 2008. In situ carbonation of peridotite for CO_2 storage. *Proceedings of the National Academy of Sciences*, 105(45): 17295–17300. DOI: https://doi.org/10.1073/pnas.0805794105

Koike, K, Nagano, S and **Kawaba, K.** 1998. Construction and analysis of interpreted fracture planes through combination of satellite-image derived lineaments and digital elevation model data. *Computers & Geosciences*, 24(6): 573–583. DOI: https://doi.org/10.1016/S0098-3004(98)00021-1

Kopp, C, Fruehn, J, Flueh, ER, Reichert, C, Kukowski, N, Bialas, J and **Klaeschen, D.** 2000. Structure of the Makran subduction zone from wide-angle and reflection seismic data. *Tectonophysics*, 329(1): 171–191. DOI: https://doi.org/10.1016/S0040-1951(00)00195-5

Kusky, T, Robinson, C and **El-Baz, F.** 2005. Tertiary-Quaternary faulting and uplift in the northern Oman Hajar Mountains. *Journal of the Geological Society*, 162(5): 871–888. DOI: https://doi.org/10.1144/0016-764904-122

Kwarteng, AY, Dorvlo, AS and **Vijaya Kumar, GT.** 2009. Analysis of a 27-year rainfall data (1977–2003) in the Sultanate of Oman. *International Journal of Climatology*, 29(4): 605–617. DOI: https://doi.org/10.1002/joc.1727

Le Métour, J, de Gramont, X and **Villey, M.** 1986. Geological Map – Quryat 1: 100.000. Sheet NF 40-4D. Muscat: Ministry of Petroleum and Minerals, Sultanate of Oman.

Malvoisin, B. 2015. Mass transfer in the oceanic lithosphere: serpentinization is not isochemical. *Earth and Planetary Science Letters*, 430: 75–85. DOI: https://doi.org/10.1016/j.epsl.2015.07.043

Mauz, B, Vacchi, M, Green, A, Hoffmann, G and **Cooper, A.** 2015. Beachrock: a tool for reconstructing relative sea level in the far-field. *Marine Geology*, 362: 1–16. DOI: https://doi.org/10.1016/j.margeo.2015.01.009

Mervine, EM, Humphris, SE, Sims, KWW, Kelemen, PB and **Jenkins, WJ.** 2014. Carbonation rates of peridotite in the Samail Ophiolite, Sultanate of Oman, constrained through ^{14}C dating and stable isotopes. *Geochimica et Cosmochimica Acta*, 126: 371–397. DOI: https://doi.org/10.1016/j.gca.2013.11.007

Moraetis, D, Mattern, F, Scharf, A, Frijia, G, Kusky, TM, Yuan, Y and **El-Hussain, I.** 2018. Neogene to Quaternary uplift history along the passive margin of the northeastern Arabian Peninsula, eastern Al Hajar Mountains, Oman. *Quaternary Research*, 90(2): 1–17. DOI: https://doi.org/10.1017/qua.2018.51

Musson, RMW. 2009. Subduction in the Western Makran. The historian's contribution. *Journal of the Geological Society*, 166(3): 387–391. DOI: https://doi.org/10.1144/0016-76492008-119

Opdyke, ND, Spangler, DP, Smith, DL, Jones, DS and **Lindquist, RC.** 1984. Origin of the epeirogenic uplift of Pliocene-Pleistocene beach ridges in Florida and development of the Florida karst. *Geology*, 12(4): 226–228. DOI: https://doi.org/10.1130/0091-7613(1984)12<226:OOTEUO>2.0.CO;2

Parker, AG. 2010. Pleistocene climate change in Arabia: developing a framework for hominin dispersal over the last 350 ka. In: Petraglia, MD and Rose, JI (eds.), *The evolution of human populations in Arabia*, 39–49. Dordrecht: Springer. DOI: https://doi.org/10.1007/978-90-481-2719-1_3

Poole, AJ and **Robertson, AHF.** 1991. Quaternary uplift and sea-level change at an active plate boundary, Cyprus. *Journal of the Geological Society*, 148(5): 909–921. DOI: https://doi.org/10.1144/gsjgs.148.5.0909

Rabu, D, Le Metour, J, Bechennec, F, Beurrier, M, Villey, M and **Bourdillon-de-Grissac, C.** 1990. Sedimentary aspects of the Eo-Alpine cycle on the northeast edge of the Arabian Platform (Oman Mountains). In: Robertson, AHF, Searle, MP and Ries, AC (eds.), *The*

Geology and Tectonics of the Oman Region, 49–68. London: Geological Society of London Special Publication 49. DOI: https://doi.org/10.1144/GSL.SP.1992.049.01.05

Rajendran, S and **Nasir, S.** 2014. ASTER mapping of limestone formations and study of caves, springs and depressions in parts of Sultanate of Oman. *Environmental earth sciences*, 71(1): 133–146. DOI: https://doi.org/10.1007/s12665-013-2419-7

Ramasamy, SM, Kumanan, CJ, Selvakumar, R and **Saravanavel, J.** 2011. Remote sensing revealed drainage anomalies and related tectonics of South India. *Tectonophysics*, 501(1): 41–51. DOI: https://doi.org/10.1016/j.tecto.2011.01.011

Rodgers, DW and **Gunatilaka, A.** 2003. Bajada formation by monsoonal erosion of a subaerial forebulge, Sultanate of Oman. *Sedimentary Geology*, 154(3): 127–146. DOI: https://doi.org/10.1016/S0037-0738(02)00126-4

Rodriguez, M, Fournier, M, Chamot–Rooke, N, Huchon, P, Bourget, J, Sorbier, M, Zaragosi, S and **Rabaute, A.** 2011. Neotectonics of the Owen Fracture Zone (NW Indian Ocean): Structural evolution of an oceanic strike-slip plate boundary. *Geochemistry, Geophysics, Geosystems*, 12(12). DOI: https://doi.org/10.1029/2011GC003731

Rose, JI, Hilbert, YH, Usik, VI, Marks, AE, Jaboob, MMA, Černý, V, Crassard, R and **Preusser, F.** 2019. 30,000-Year-Old Geometric Microliths Reveal Glacial Refugium in Dhofar, Southern Oman. *Journal of Paleolithic Archaeology*. DOI: https://doi.org/10.1007/s41982-019-00027-3

Rougeulle, A. 2017. Medieval Qalhāt, historical vs archaeological data. *Arabian Humanities. Revue internationale d'archéologie et de sciences sociales sur la péninsule Arabique/International Journal of Archaeology and Social Sciences in the Arabian Peninsula*, (9). DOI: https://doi.org/10.4000/cy.3442

Rougeulle, A, Renel, H, Simsek, G and **Colomban, P.** 2014. Medieval ceramic production at Qalhāt, Oman, a multidisciplinary approach. *Proceedings of the Seminar for Arabian Studies*, 44: 299–315.

Schuiling, RD. 2011. Troodos: a giant serpentinite diapir. *International Journal of Geosciences*, 2(2): 98. DOI: https://doi.org/10.4236/ijg.2011.22010

Searle, MP. 2007. Structural geometry, style and timing of deformation in the Hawasina Window, Al Jabal al Akhdar and Saih Hatat culminations, Oman Mountains. *GeoArabia-Manama*, 12(2): 99–130.

Searle, MP and **Cox, J.** 1999. Tectonic setting, origin, and obduction of the Oman ophiolite. *Geological Society of America Bulletin*, 111(1): 104–122. DOI: https://doi.org/10.1130/0016-7606(1999)111<0104:TSOAOO>2.3.CO;2

Smith, GL, McNeill, LC, Wang, K, He, J and **Henstock, TJ.** 2013. Thermal structure and megathrust seismogenic potential of the Makran subduction zone. *Geophysical Research Letters.* 40(8): 1528–33. DOI: https://doi.org/10.1002/grl.50374

Smith, MJ and **Pain, CF.** 2009. Applications of remote sensing in geomorphology. *Progress in Physical Geography*, 33(4): 568–582. DOI: https://doi.org/10.1177/0309133309346648

Stewart, SA. 2006. Implications of passive salt diapir kinematics for reservoir segmentation by radial and concentric faults. *Marine and Petroleum Geology*, 23(8): 843–853. DOI: https://doi.org/10.1016/j.marpetgeo.2006.04.001

Streit, E, Kelemen, P and **Eiler, J.** 2012. Coexisting serpentine and quartz from carbonate-bearing serpentinized peridotite in the Samail Ophiolite, Oman. *Contributions to Mineralogy and Petrology*, 164(5): 821–837. DOI: https://doi.org/10.1007/s00410-012-0775-z

Vita-Finzi, C. 2001. Neotectonics at the Arabian plate margins. *Journal of Structural Geology*, 23(2): 521–530. DOI:https://doi.org/10.1016/S0191-8141(00)00117-6

Warren, CJ, Parrish, RR, Waters, DJ and **Searle, MP.** 2005. Dating the geologic history of Oman's Semail ophiolite. Insights from U-Pb geochronology. *Contributions to Mineralogy and Petrology*, 150(4): 403–422. DOI: https://doi.org/10.1007/s00410-005-0028-5

Wessel, B. 2016. TanDEM-X Ground Segment-DEM Products Specification Document. Public Document TD-GS-PS-0021, no. 3.0, 2013.

Withjack, MO and **Scheiner, C.** 1982. Fault patterns associated with domes-an experimental and analytical study. *AAPG Bulletin*, 66(3): 302–316. DOI: https://doi.org/10.1306/03B59AFD-16D1-11D7-8645000102C1865D

Woo, HB, Panning, M, Adams, PN and **Dutton, A.** 2017. Flexural isostasy of the carbonate platform in North central Florida. *Geochemistry, Geophysics, Geosystems*, 18(9): 3327–3339. DOI: https://doi.org/10.1002/2017GC006934

Wyns, R, Béchennec, F, Le Métour, J and **Roger, J.** 1992. Geological Map – Tiwi 1: 100.000. Sheet NF 40–8B. Muscat: Ministry of Petroleum and Minerals, Sultanate of Oman.

Yuan, Y, Kusky, TM and **Rajendran, S.** 2016. Tertiary and quaternary marine terraces and planation surfaces of northern Oman. Interaction of flexural bulge migration associated with the Arabian-Eurasian collision and eustatic sea level changes. *Journal of Earth Science*, 27(6): 955–970. DOI: https://doi.org/10.1007/s12583-015-0656-2

Zink, M, Bartusch, M and **Miller, D.** 2011. TanDEM-X mission status. *Geoscience and Remote Sensing Symposium (IGARSS), 2011 IEEE International*. IEEE, 2290–2293. DOI: https://doi.org/10.1109/IGARSS.2011.6049666

Zink, M, Fiedler, H, Hajnsek, I, Krieger, G, Moreira, A and **Werner, M.** 2006. The TanDEM-X mission concept. *Geoscience and Remote Sensing Symposium (IGARSS), 2006 IEEE International*. IEEE, 1938–1941. DOI: https://doi.org/10.1109/IGARSS.2006.501

How to cite this article: Ermertz, AM, Kázmér, M, Adolphs, SK, Falkenroth, M and Hoffmann, G. 2019. Geoarchaeological Evidence for the Decline of the Medieval City of Qalhat, Oman. *Open Quaternary*, 5: 8, pp. 1–14. DOI: https://doi.org/10.5334/oq.56

Submitted: 30 January 2019 **Accepted:** 06 September 2019 **Published:** 27 September 2019

]u[*Open Quaternary* is a peer-reviewed open access journal published by Ubiquity Press. OPEN ACCESS